World Environment 2015, 5(1): 17-27
DOI: 10.5923/j.env.20150501.03

Comparison of UV Index from EP/TOMS with Ground-Based Measurements at Subtropical Location

Abdel Galeil. A. Hassan

Physics Department, Faculty of Science, South Valley University, Qena, Egypt

Abstract The purpose of the UV Index estimation is to help people effectively protect themselves from UV radiation, of which excessive exposure causes sunburn. UV index (UVI) has been estimated in Qena, Upper Egypt (26°17' N, 32°43' E, 97 m asl) at noon during the period (Apr. 2000 - Dec. 2005) using EP/TOMS satellite (UVI_{sat}) and ground-based measurements (UVI_{grd}). Temporal variations of UVI_{sat} and UVI_{grd}, also, comparison between them have been investigated. In addition, the effect of atmospheric conditions, in the form of cloud cover and aerosol index, on this comparison has been analyzed. The study revealed that, in all sky conditions, average value of UVI_{sat} and UVI_{grd} were 9.39±2.60 and 8.1±2.4, respectively. While, in cloudless conditions (cloud cover CC = 0 oct.), their values became 9.98±2.39 and 8.53±2.10, respectively. In addition, the value that has more occurrence for UVI_{sat} and UVI_{grd}, in both conditions (all sky and cloudless conditions), was 12 and 10, respectively. Regarding the comparison between UVI_{sat} and UVI_{grd}, effects of clouds and aerosols were taken into consideration. So that, four data subsets were analyzed, subset 1: all sky conditions, subset 2: all cloudless cases, subset 3: cloudless cases with low aerosol index and subset 4: cloudy cases with low aerosol index. The study showed that UVI_{sat} values were higher than the UVI_{grd} during all studied period under all studied conditions. The largest biases were found on heavy overcast days (positive biases reached to 42%).

Keywords UV index, EP/TOMS, UVB-1 Pyranometer, Clouds, Aerosol index, Qena, Egypt

1. Introduction

UV radiation can be subdivided physically according to wavelength into four divisions, mainly near UV (320–400 nm), middle UV (280–320 nm), far UV (200–280 nm), vacuum and extreme UV (100–200 nm) [1-3] Although, in the outer space, UV-A and UV-B represent about 7.5% of the total solar irradiance, at the earth's surface typically make up between 3% and 5% of the solar total irradiance [4].

In the last years, the erythema has received most attention. Thus, this effect is commonly quantified weighting the solar UV radiation with the erythemal spectral response, resulting in the so called erythemal ultraviolet irradiance (EUV). In 1987 Commission Internationale de l'Eclairage (CIE), adopted curve relating UV irradiance and erythemal action spectrum currently recommended as the standard erythemal action spectrum. Therefore, the variable EUV is recognized internationally as a standard for determining the risk associated to UV radiation [5, 6]. The UV Index (UVI) has been recommended by several international organizations such as: World Meteorological Organization (WMO), World Health Organization (WHO), United Nations Environment Program (UNEP) and International Commission on Non-Ionizing Radiation (ICNIRP) as a useful tool to inform the public about the magnitude of the EUV at the earth's surface in order to protect themselves against the potentially harmful effects of the UV radiation. The UVI is determined by multiplying EUV (expressed in W/m^2) by 40 according to the joint recommendation of the WMO, WHO, UNEP and ICNIRP meeting on UV-B radiation and UV forecast in July 1997. For the general public it is usually given as an integer number, i.e. without decimals. UV intensity is described in terms of ranges running from low values (less than 2), moderate (3–5), high (6–7), very high (8–10) and extreme (11^+). The clear sky value at sea level in the tropics is normally in the range 10–12 and 10 is an exceptionally high value for northern mid-latitudes.

The continuous validation of satellite EUV data with ground-based measurements from well-calibrated and well-maintained instruments is an essential task for assessing the quality and accuracy of satellite data and to identify local to regional specific sources of uncertainty [7, 8]. Comparison between EUV at noon in mW/m^2 from Total Ozone Mapping Spectrometer (TOMS) instruments with ground measurements has been studied by many authors [9-18] Most of these works revealed that the satellite UV data overestimate the ground-based measurements in many locations.

Anton et al., 2007 [19] found that the TOMS retrievals of

* Corresponding author:
hassan_xp58@yahoo.com (Abdel Galeil. A. Hassan)
Published online at http://journal.sapub.org/env

noon EUV irradiance compared with Brewer ground-based measurements under different sky conditions showed that TOMS overestimates the EUV data by 12% during cloud-free days, and the bias increases with the aerosol load. The comparison of EUV intensities on a normal day and on a day with high aerosol loading suggests about 24% decrease in EUV amounts on the day with high aerosol loading [19] Palancar and Toselli, (2002) [20] implied that cloud cover (CC) and aerosol loads are major factors in the UV depletion. Clouds can significantly reduce UV-B radiation if cloud cover is greater than 50% [21]. Also, Frederick and Snell, (1990) were found that the erythemal irradiance annual mean is reduced between 22% and 38% relative to the clear sky value by clouds [22].

It has been shown by ground-based measurements that large reductions of UV-B occur under absorbing aerosols such as smoke from biomass burning [23-24], forest fires [25] or desert dust [26]. Kazadzis et al., (2009) found that compared UV irradiance products from OMI against ground-based Brewer measurements, showing that OMI overestimates UV spectral irradiances by 30%, 17% and 13% for 305 nm, 324 nm, and 380 nm, respectively [27]. Also, Ialongo et al., (2008) [12] showed that OMI UV data overestimate ground-based EUV values measured from both Brewer spectrophotometer and YES broadband radiometer (biases about 20%) [36] at Rome (Italy). Weihs et al., (2008) showed that OMI-Brewer differences can reach +50% under overcast conditions [18] during a validation campaign in the region of Vienna (Austria). In upper Egypt, El-Shazly et al., (2012) studied UVI in 10 locations, including Qena, and created an empirical model for estimation UVI in all sky conditions using solar declination, solar zenith angle, total ozone column, reflectivity and aerosol index as independent variables [28].

This paper aims at compare the derived UV index from EP/TOMS (UVI_{sat}) with the derived UV index by UVB-1 Ultraviolet Pyranometer (UVI_{grd}) at Qena, Upper Egypt (26°17' N, 32°43' E, 97 m asl), see Figure (1). The period of study extended from April 2000 to December 2005. The effects of clouds and aerosols on these comparisons will be analyzed using four atmospheric conditions used by Anton et al., (2010) [38]. For studying the effect of aerosols we used the data of aerosol index (AI) instead of aerosol optical depth used by them.

2. Location Description

Qena City (26°17' N, 32°43' E, 97 m asl) is located in Upper Egypt, about 600 Km south of Cairo and 60 Km north of Luxor (Figure 1). It located mainly within the narrow Nile valley which separates Egypt to two unequal dessert parts, the western and the eastern deserts. The climate of Qena is characterized by very hot and dry summer season with average daily maximum temperature T = 40℃ and average daily minimum RH = 17%, cold winter with average daily maximum temperature T = 25 and average daily minimum RH = 26% [30]. It rarely rains. It receives large quantity of solar radiation, especially in summer [29].

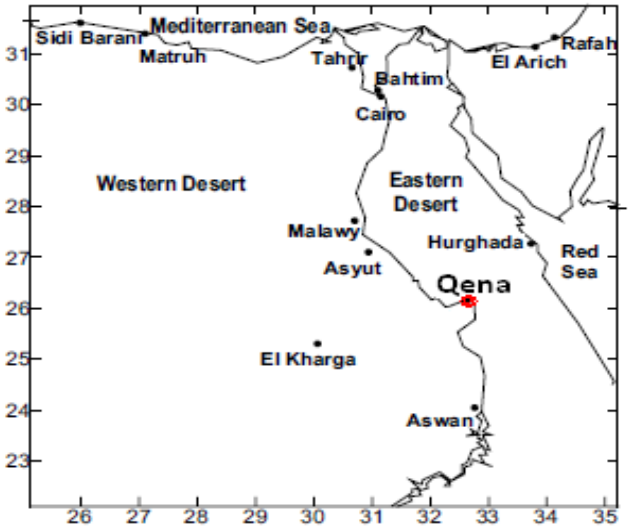

Figure 1. The studied area, Qena, Egypt

3. Description of Satellite and Ground Based Measurements

3.1. Satellite Observations

The Total Ozone Mapping Spectrometer (TOMS) instrument developed by National Aeronautics and Space Administration (NASA) Goddard Space Flight Center (GSFC) was designed to enable long-term daily mapping of global distribution of the earth's atmospheric ozone. TOMS makes 35 measurements every 8 seconds each covering a width of 30 to 125 miles (50-200 km) on the ground, strung along a line perpendicular to the satellite path motion. TOMS uses the ratio of back scattered earth radiance to solar irradiance at specific wavelength to infer total ozone [31]. Earth Probe/Total Ozone Mapping Spectrometer (EP/TOMS) was launched July 2, 1996 and the first full day of data file generation began on July 25, 1996. It provided continuous data from that time until December 2005, with the exception of a few days in Dec 1997 during which the satellite orbit was boosted from 500km to 750km, and a period in late 1998 when the instrument was in Safe hold [32].

3.1.1. Erythemal Noontime Irradiance

Data used for determination of UVI_{sat} is the erythemal noontime irradiance measured by (EP/TOMS) in a 1x1.25 degree grid in units of milli-watts/m^2/nm which is available in ftp://toms.gsfc.nasa.gov/pub/.

The weighting function used to approximate the wavelength-dependent sensitivity of Caucasian skin to erythema-causing radiation is the model proposed by McKinlay and Diffey [33]. The UVI_{sat} is calculated using the erythemal (CIE) action spectrum. It is non-dimensional, obtained by dividing the CIE-weighted integral by 25 mWm^{-2} [34].

3.1.2. Reflectivity (reflc.) in % and Effective Cloud Fraction

The solar irradiance reflected up to a spacecraft from the surface of the Earth can be used to calculate reflectivity. Reflected radiation can come from two surfaces, the ground, and the tops of clouds. Reflectivity is determined from the measurements at 360 nm in the case of Earth Probe. For a given TOMS measurement, the first step is to determine calculated radiance at 360 nm for reflection off the ground and reflection from cloud, based on the tables of calculated 360-nm radiance. For reflection from the ground, the terrain height pressure is used, and the reflectivity is assumed to be 0.08. For cloud radiance, a pressure corresponding to the cloud height from the International Satellite Cloud Climatology Project (ISCCP) based climatology is used, and the reflectivity is assumed to be 0.80 [32]. The ground radiance (I_{ground}) and cloud radiance (I_{cloud}) are then compared with the measured radiance $I_{measured}$. If $I_{ground} \leq I_{measured} \leq I_{cloud}$, and snow/ice is assumed not to be present, an effective cloud fraction f is derived using

$$f = \frac{I_{measured} - I_{ground}}{I_{cloud} - I_{ground}} \quad (1)$$

Data of reflectivity is available in ftp://toms.gsfc.nasa.gov/pub/eptoms.

3.1.3. Aerosol Index (AI)

The TOMS technique of aerosol detection and characterization is based on spectral contrast in the UV that results from the interaction between the processes of Rayleigh scattering, particle scattering and absorption. This interaction produces spectral variations of the back scattered radiance at the top of the atmosphere that can be used to separate aerosol absorption from scattering effects. Torres et al. (1998) discuss in detail the physical basis of the near UV technique of aerosol sensing [35]. The TOMS aerosol index is a measure of how much the wavelength (λ) dependence of back scattered UV radiation from an atmosphere containing aerosols (Mie scattering, Rayleigh scattering, and absorption) differs from that of a pure molecular atmosphere (pure Rayleigh scattering). AI for EP/TOMS is defined as (Hsu et al., 1999) [43].

$$\mathrm{AI} = -100\left\{\log_{10}\left(\frac{\lambda_{331}}{\lambda_{330}}\right)_{mes} - \log_{10}\left(\frac{\lambda_{331}}{\lambda_{330}}\right)_{calc}\right\} \quad (2)$$

Where subscript mes indicates the measured back scattered radiance at the fixed wavelength and subscript calc indicates calculated using RT model describing a pure Rayleigh atmosphere [35]. Data of aerosol index is available in fttp://toms.gsfc.nasa.gov/pub/eptoms /overpass/

3.2. Ground-based Measurements and Calculation of UVI_{grd}

Cloud cover in Oktas and noon time total irradiance from 280 to 320 nm (UV-B) are measured in South Valley University (SVU)-meteorological research station in Qena/Upper Egypt, during the period (Apr. 2000- Dec.2005). UV-B irradiance is measured by a precision radiometer UVB-1. The instrument's innovative measurement technique uses colored glass filters and a UV-B phosphor to convert incoming UV-B radiation to green light, which is then measured by a calibrated solid state photo detector (YES, 2008) [36]. Hourly values measurements of UV-B at the horizontal surface at noon time were carried out. The Model UVB-1 Ultraviolet Pyranometer ‘‘No. 960842, Yankee Environmental Systems Inc. (YES) was used to measure the total irradiance from 280 to 320 nm (UV-B), its cosine response is ±5% for 0 – 60 degrees solar zenith angle and its sensitivity is 1.97 (watt/m^2)/volt of total UV-B irradiance. The hourly values of UV-B were recorded by Compilog Data logger (No. 1020, TH. Friedrichs & CO. ‘‘Germany’’).

The UVB-1 instrument output voltage is converted to the CIE-defined erythemal irradiance in effective mW/m^2 through multiplying the signal voltage by the conversion factor corresponding to the appropriate solar zenith angle (YES, (1997) [37, 33]. UVI_{grd}, can then be calculated by dividing the resulted erythemal values by 25.

4. Methodology

To select cloud-free conditions, the EP/TOMS Reflectivity (reflc.) was used. Thus, a day is considered cloud-free during (reflc.) is lower than 10% [13]. The percentage of such cloud-free days was about 64% of the total amount of days at Qena/Upper Egypt during the study period. Aerosol events were identified according to the aerosol index (AI), obtain from EP/TOMS data (NASA, 2011b) [39]. To investigate the effect of clouds and aerosols on the EP/TOMS bias, the following four datasets were analyzed:

Dataset 1: all sky conditions.
Dataset 2: all cloudless cases (reflc. <10%).
Dataset 3: cloudless cases with low aerosol index (reflc. <10% and AI<1).
Dataset 4: cloudy cases with low aerosol index (reflc. >10% and AI<1).

Regression analysis was performed separately for each dataset and statistics analysis have been done to calculate the mean bias error (MBE), the mean absolute bias error (MABE) and root mean square error (RMSE). These statistics are obtained by the following expressions:

$$MBE\ (\%) = 100 \cdot \frac{1}{n}\sum_{i=1}^{n}\frac{UVI_{sat} - UVI_{grd}}{UVI_{sat}} \quad (3)$$

$$MABE(\%) = 100 \cdot \frac{1}{n}\sum_{i=1}^{n}\frac{\left|UVI_{sat} - UVI_{grd}\right|}{UVI_{sat}} \quad (4)$$

$$RMSE\ (\%) = \left[\frac{1}{n} \sum_{i=1}^{n} \left(\frac{UVI_{sat} - UVI_{grd}}{UVI_{sat}} \right)^2 \right]^{0.5} \quad (5)$$

For considering the different number of data used in each dataset, the uncertainty of MBE and MABE is characterized by the standard error (SE), defined as:

$$SE = \frac{SD}{\sqrt{n}} \quad (6)$$

where SD is the standard deviation and *n* is the number of data in each dataset.

5. Results and Discussion

5.1. Daily Variation of UVI_{sat} and UVI_{grd}

The calculated daily average variation of UVI_{sat} and UVI_{grd} at noon time during the period (Apr. 2000- Dec. 2005) in both all sky conditions and cloudless conditions (CC= 0 Oct) is depicted in Figure (2). Generally, the same behavior is found for the two variables. It attained low values at winter months, and increased to high values at summer months, after that it decreased to record low values at autumn months.

The values of UVI_{grd} were lower than that of UVI_{sat} in both of all sky conditions and cloudless conditions as shown in Table (1), This result is found by Ialongo et al., 2008, where, they have been studied the comparison of erythemal UV data from OMI with ground-based measurements, they showed that OMI EUV data overestimates ground-based EUV values measured from both Brewer spectrophotometer and YES broadband radiometer (biases about 20%) at Rome (Italy) [12]. This low estimation can be attributed to differences in spatial resolution between the two methods, ground based and satellite, of measuring EUV as well as the effect of atmospheric conditions.

Table 1. Average, maximum average and minimum average of UVI_{sat} and UVI_{grd} in all sky conditions and cloudless sky conditions calculated at noon time during the period (Apr. 2000- Dec. 2005)

	All sky conditions		Cloudless sky conditions	
	UVI_{sat}	UVI_{grd}	UVI_{sat}	UVI_{grd}
Average	9.39±2.60	8.1±2.41	9.98±2.39	8.53±2.10
Max. avg.	12.60	11.92	12.60	11.92
Minim. avg.	4.71	3.97	3.68	3.97

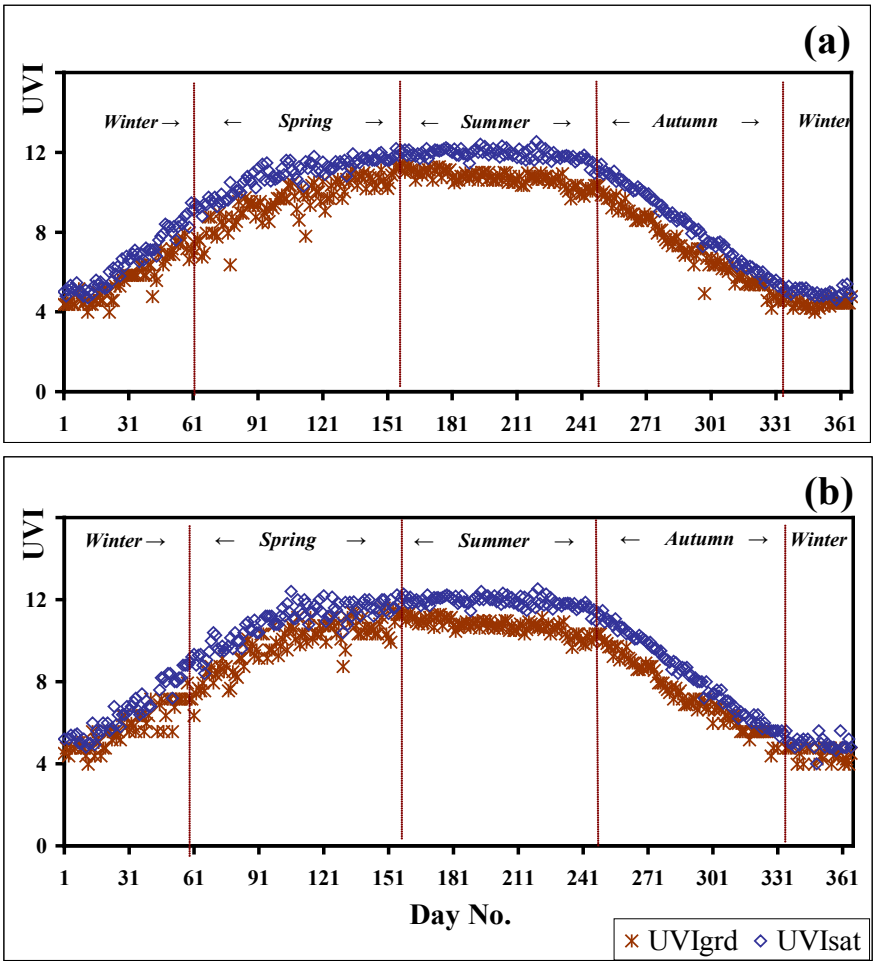

Figure 2. Daily average variation of UVI_{sat} and UVI_{grd} at Qena/Upper Egypt (Apr.2000-Dec.2005) in (a) all sky conditions and (b) cloudless sky condition

5.2. Frequency of Daily UVI Values

The frequency of UVI_{sat} and UVI_{grd} values are discussed in all sky conditions and cloudless conditions for determining which value of UVI has more occurrences in our area. The frequency distribution showed that the UVI_{sat} with value of 12, which is considered as extreme, had more occurrences in both conditions, Figure (3), where their frequencies were 30.1% and 37.2% in all sky conditions and cloudless conditions, respectively. According to the EPA general guidelines UV levels are dangerous; one must be extra careful outdoors, where, unprotected skin can burn in minutes.

In the other hand, UVI_{grd} frequency distribution showed that the UVI_{grd} with value of 10, which is considered as very high, have more occurrence in all sky conditions and cloudless conditions, where their frequencies were 29.5% and 33.9%, respectively, as shown in Figure (4). According to the EPA general guidelines UV levels are dangerous and extra precautions must be considered, where, in this case, unprotected skin will be damaged and can burn quickly.

5.3. Comparison between UVI_{sat} and UVI_{grd}

Figure (5) shows the scatter plot between UVI_{sat} and UVI_{grd} in all the aforementioned data sets during the period of study (April 2000–December 2005). The results of linear regression analysis between UVI_{sat} and UVI_{grd} for all datasets, including, the slope of the regression, the standard error (SE) of the slope, the Y intercept, the SE of the Y intercept and the correlation coefficients (r) are presented in Table (2).

Table 2. The results of linear regression analysis between UVI_{sat} and UVI_{grd} for all datasets

Dataset	Slope	SE (Slope)	Y intercept	SE (Y intercept)	r (%)
Dataset 1: (All conditions)	0.9673±0.012	0.000	1.4189v0.108	0.004	88.5
Dataset 2: (CC=0 reflc<10%)	0.9778±0.014	0.001	1.3079±0.139	0.006	88.8
Dataset 3: (CC=0 reflc<10% AI<1)	1.0780±0.028	0.002	0.5104±0.219	0.019	92.2
Dataset 4: (CC≥1 reflc>10% AI<1)	1.1569±0.098	0.017	0.2557±0.576	0.100	81.1

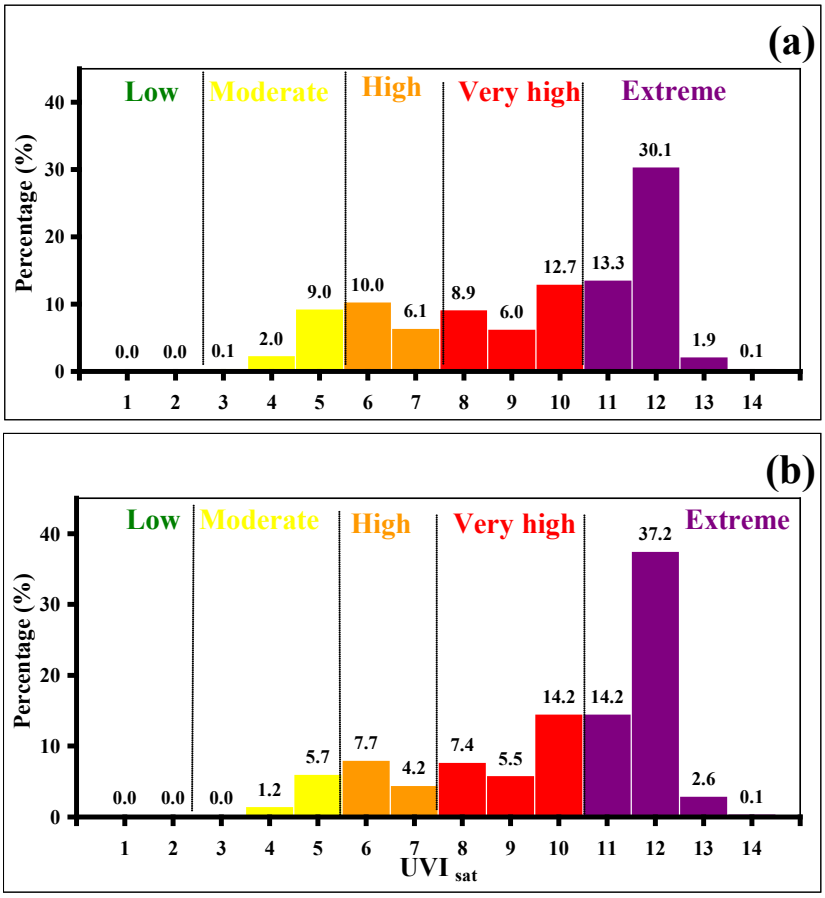

Figure 3. Frequency of UVI_{sat} at Qena/Upper Egypt (Apr.2000-Dec.2005) in (a) all sky conditions and (b) cloudless condition

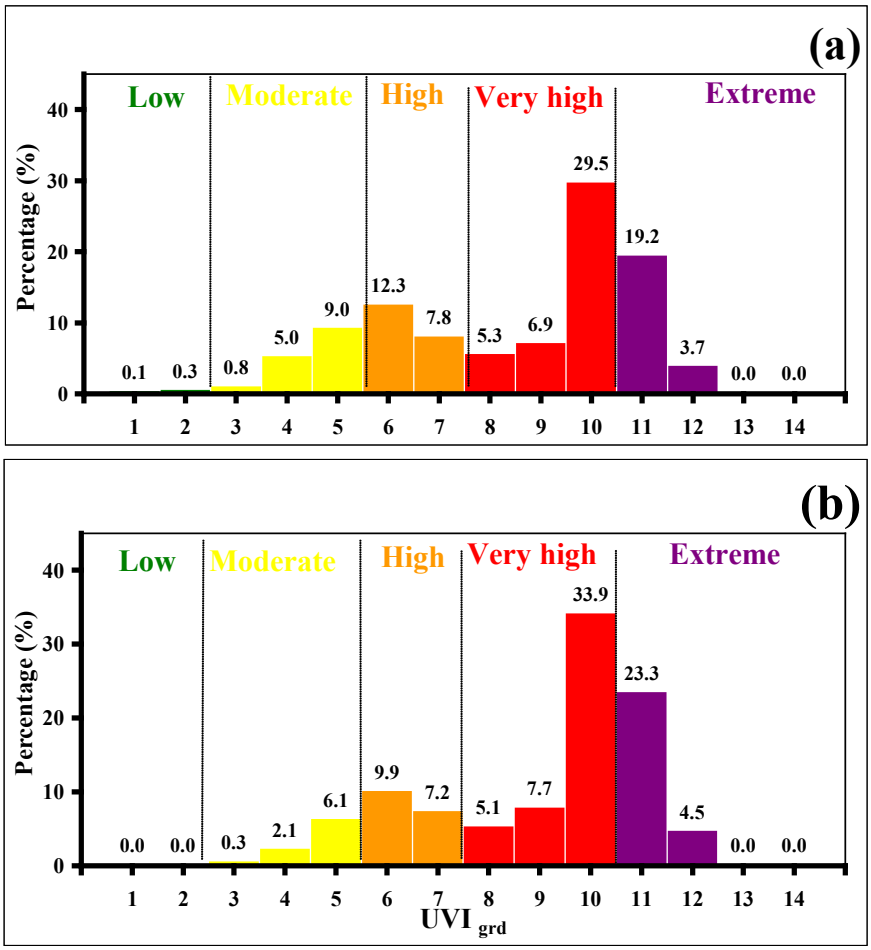

Figure 4. Frequency of UVI_{grd} at Qena/Upper Egypt (Apr.2000-Dec.2005) in (a) all sky conditions and (b) cloudless condition

5.3.1. Data Set 1: All Sky Conditions

The data set1 are characterized with all sky conditions. UVI_{sat} were compared with UVI_{grd} in 950 days during the study period. The comparison is shown in Table (2) as well as Figure (5a). Regression analysis between UVI_{sat} and UVI_{grd} showed positive linear relationship characterized by regression slope of 0.967±0.01 and intercept equals to 1.4189. The RMSE and correlation coefficient were 34.77±0.05 and 0.941, respectively. The regression formula was:

$$UVI_{sat} = 0.9673UVI_{grd} + 1.4189 \quad (7)$$

Scatter plot between MBE% and day number illustrated that MBE% was less than 30%. Table (3) showed positive sign of both MBE and MABE which means that UVI_{sat} overestimate UVI_{grd}. This overestimation was (11.85±0.09)%. Also, MABE parameter was (12.19±0.09)%. The uncertainty SE of this last parameter was 0.003 %, indicated the statistical significance of the values. Also, the RMSE attained the value (34.77±0.1)% with standard error (0.001)%.

This overestimation may be attributed to uncertainty in satellite-derived UV that is probably related to the inability of the satellite sensors to correct for boundary layer extinctions. Ground-based estimates of regional UV irradiances suffer from a similar inability to correct for horizontal in homogeneities in boundary layer extinction as well as in homogeneities in the troposphere and stratosphere.

Overestimation of UVI_{sat} on UVI_{grd} can also be explained by the fact that there are differences in spatial resolution between the two methods of measuring erythemal UV by ground based and satellite. The field of view of satellite measurement is about 100 km while the ground based instrument has a smaller field of view. Temporal differences can also occur because of difference in measuring time, as TOMS data are recorded during the time of direct overpass of the location, while ground-based measurements are recorded at local noon. This explanation has been stated before by [7], [40] and [41].

Also, overestimation of UVI_{sat} on UVI_{grd} can be explained by the effect of cloud covers where the result shows that The MBE and MABE have relatively large values, on heavy overcast days reached up to 19.34±0.18 and 19.69±0.17, respectively. (Effect of cloud will be discussed latter in cloudy case). Aerosol contents in the atmosphere also, play an important role for the relative difference between the ground-based and satellite measurements of EUV irradiation.

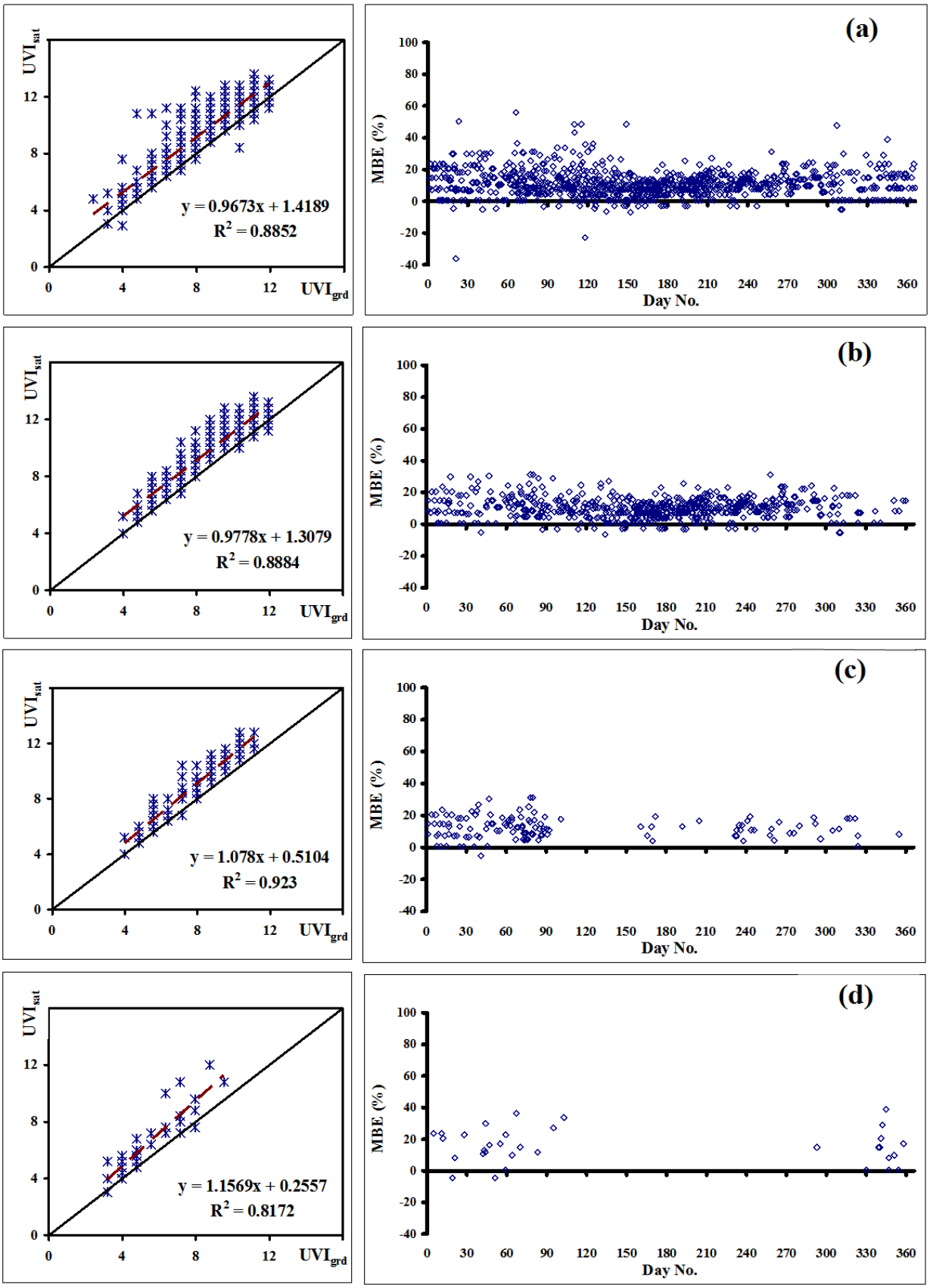

Figure 5. In the left side, scatter plot between UVI_{sat} and UVI_{grd} for each dataset. In the right side, scatter plot between MBE% and day number for each dataset: (a) for dataset 1; (b) for dataset 2; (c) for dataset 3 and (d) for dataset 4. The dashed line is the least square linear regression line, and the solid line symbolizes the ideal correlation of unit slope

Table 3. Values of data number (N) and its ratio of the total days (%), also MBE, MABE, RMSE and SE for the values of UVI_{sat} and UVI_{grd} for all datasets during the period (Apr. 2000 - Dec. 2005)

Dataset	N	% of total days	MBE (%)	SE (*MBE*)	MABE (%)	RMSE (%)	SE (*RMSE*)
Dataset 1: (All conditions)	950	100	11.85±0.09	0.003	12.19±0.09	34.77±0.1	0.001
Dataset 2: (reflc.<10%)	608	64	10.44±0.1	0.003	10.66±0.1	27.63±0.0	0.001
Dataset 3: (reflc.<10% AI<1)	104	11	13.04±0.1	0.007	13.14±0.1	11.49±0.0	0.002

5.3.2. Data Set 2: Cloud-free Conditions

For studying the effect of aerosols, data set 2 are characterized with reflc <10%, including all values of AI. The calculated UVI_{sat} were compared with UVI_{grd} in 608 days representing the 64% of all days within the analyzed period. The result of the comparison is shown in Table (2) as will as Figure (5b). The regression analysis showed positive relationship between UVI_{sat} and UVI_{grd} which characterized by regression slope of 0.9778±0.01 and intercept of 1.3079 with correlation coefficient 0.943. *i.e.* in the form:

$$UVI_{sat} = 0.9778UVI_{grd} + 1.3079 \quad (8)$$

Scatter plot between MBE% and day number illustrated that MBE% was less than 20% most of the year. Also, the results showed an overestimate of UVI_{sat} on UVI_{grd} as shown in Table (3). This overestimation was (10.44±0.07) %, lower than that in all sky conditions. SE of this parameter was 0.003 %. In addition, the MABE parameter decreased to be (10.66+0.09)%. Also, RMSE decreased to (27.63±0.0)%. Compared with the data set1 (all sky conditions), the data noise is relatively decreased and the correlation was higher. This finding may be related to the absence of the cloudiness compensating effect occurred for data set 1. The relative differences between the UVI_{sat} and UVI_{grd} may be, due to the effect of aerosol contents in the atmosphere. These encouraged us to draw a relation between the average values of MBE (%) and AI as shown in figure (6). It is clear that the MBE increases as increasing the AI. The empirical formula was in the form:

$$MBE(\%) = 1.5948(AI)^2 - 5.9186(AI) + 15.576 \quad (9)$$

This result is found by Kim et al., 2008, where, they have been studied the determination of radiation amplification factor (RAF) of atmospheric aerosol [42] from the surface UV irradiance measurement. Value of the RAF of aerosols for UV-B ranged from - 0.22 to - 0.26. Also, the comparison of EUV intensities on a normal day and on a day with high aerosol loading suggested about 24% decrease in EUV amounts on the day with high aerosol loading [19] in India.

Also, figure (6) shows that, for AI ≥3.6, more variation between UVI_{sat} and UVI_{grd}. This is may be attributed to more aerosol concentration, of which occur during unstable weather conditions.

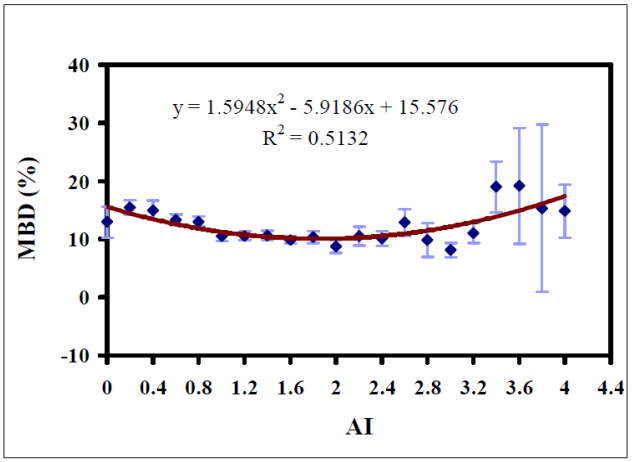

Figure 6. The effects of AI on MBE (%) between UVI_{sat} and UVI_{grd} (Apr.2000-Dec.2005) respect to dataset 2 (vertical lines shows SE)

5.3.3. Data Set 3: Cloud-free Conditions with Low Aerosol Index

The data set 3 are characterized by (reflc. <10%) and low aerosol index (AI<1). This case covered 104 days, representing the 10.95% of all days within the analyzed period. The regression analysis parameters between the calculated UVI_{sat} and the calculated UVI_{grd} are tabulated in Table (2) and illustrated in Figure (5c). The regression analysis showed positive relation between UVI_{sat} and UVI_{grd} with slope of 1.078±0.03 and intercept of 0.5104. The correlation coefficient between UVI_{sat} and UVI_{grd} is 0.961. The relation between them is in the form:

$$UVI_{sat} = 1.078UVI_{grd} + 0.5104 \quad (10)$$

Scatter plot between MBE% and day number illustrated that MBE% was less than 20% most of the year. Table (3) showed that the calculated values of UVI_{sat} were still overestimated on UVI_{grd}. In this case, although, the MBE value was (13.04±0.07) % with SE equal 0.007 % and the MABE parameter 13.14±0.07 %, the RMSE value decreased considerably to (11.49±0.0)%. The relative differences between UVI_{sat} and UVI_{grd} in this case, may be, due to the differences in spatial resolution between the two methods of measuring EUV by ground based and satellite as explained before in dataset 1. Antón et., al 2007 in Spain studied the TOMS retrievals of noon erythemal ultraviolet irradiance

compared with Brewer ground-based measurements, they found that the comparison under different sky conditions, showed that TOMS overestimates the EUV data by 12% during cloud-free days, and the bias increases with the aerosol load [19].

5.3.4. Data Set 4: Cloudy Conditions with Low Aerosol Index

For studying the effect of clouds, the dataset 4 is characterized with reflc. > 10% and AI <1. The number of selected days of this data set is 53 days, representing 5.58% of all days within the analyzed period. The results of regression analysis are shown in Table (1) and illustrated in Figure (5d). The regression analysis shows positive relationship between UVI_{sat} and UVI_{grd}. The relation is characterized by regression slope of 1.1569±0.098 with correlation coefficients 0.904, i.e.

$$UVI_{sat} = 1.1569UVI_{grd} + 0.2557 \quad (11)$$

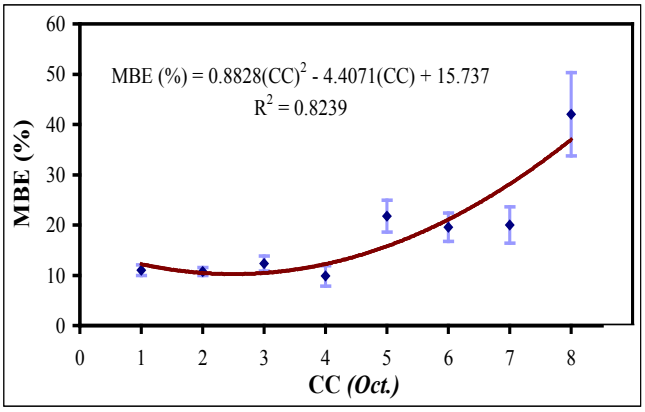

Figure 7. The effects of cloud cover (Oktas) on MBE (%) between UVI_{sat} and UVI_{grd} (Apr.2000-Dec.2005) respect to dataset 4 (vertical lines shows SE)

Scatter plot between MBE% and day number indicates that the value of MBE% is less than 30% most of the studied days. Values of MBE (%) and MABE are increased considerably to be (19.34±0.2)% and (19.69±0.2)%, respectively, as shown in Table (3) which means that UVI_{sat} overestimated UVI_{grd}. The presence of scattered or broken clouds poses difficulties for comparisons between ground-based measurements and satellite estimates of surface UV irradiance. In this situation direct solar radiation is either obscured or not obscured by a cloud at the ground-based measurement site, whereas the satellite measures an average cloud amount over its footprint [44] In the same time RMSE value decreased to be (8.54±0.1)%. The effect of CC (oct.) on MBE (%) is presented in Figure (7). Increasing disagreement caused by increasing cloud amounts stated by Silva, 2011 [45] in comparison of seasonally averaged EUV dose rate values from a ground-based instrument in Brazil with OMI overpass data. It is clear that largest deviation was found on overcast days (8 oct). This finding encouraged us to establish an empirical formula relates both CC (oct.) and the MBE (%). The empirical formula was:

$$MBE(\%) = 0.8828(CC)^2 - 4.4071(CC) + 15.737 \quad (12)$$

Weihs et al., 2008 have been studied [18] Measurements of UV irradiance within the area of one satellite pixel, they showed that OMI-Brewer differences can reach +50% under overcast conditions during a validation campaign in the region of Vienna (Austria).

6. Conclusions

The main aim of this work is the study of the derived UV index from EP/TOMS (UVI_{sat}) and the ground UV index (UVI_{grd}) obtained from UVB-1 Ultraviolet Pyranometer at Qena, Upper Egypt during the period (April 2000 to December 2005). Daily average variation of both UVI_{sat} and UVI_{grd} at noon for all days during the studied period in all sky and cloudless conditions (cloud cover CC = 0 oct.) was presented. Also, frequency distribution of UVI_{sat} and UVI_{grd} values was investigated. The effects of clouds and aerosols on comparisons between UVI_{sat} and UVI_{grd} are considered. The study leads to the following:

- Daily average value of UVI_{sat} attained the value 9.39±2.60 with maximum value of 12.60 in all sky conditions. While its average value increased to 9.98±2.39, its maximum value remained at 12.60 in cloudless conditions.
- Daily average value of UVI_{grd} attained the value 8.10±2.41 in all sky conditions and increased to 8.53±2.10 in cloudless condition, however, its maximum value was 11.92 in all sky conditions and cloudless condition.
- The UVI_{sat} with value of 12, which is considered as extreme, had more occurrence in both conditions, with frequencies 30.1% and 37.2% in all sky conditions and cloudless conditions, respectively.
- The UVI_{grd} with value of 10, which is considered as very high, has more occurrence in all sky conditions and cloudless conditions, with frequencies 29.5% and 33.9%, respectively.
- The comparison between UVI_{sat} and UVI_{grd} in all datasets showed overestimation of UVI_{sat} on UVI_{grd}. The overestimation increased with increasing cloud cover where the results show that The MBE and MABE have relatively large values on heavy overcast days.

REFERENCES

[1] Huffman Robert E., 1992: Atmospheric Ultraviolet Remote Sensing, Academic Press, Inc.

[2] Parmeggiani L., 1983: Encyclopaedia of occupational health and safety Intemational Labour Of fice, Geneva Switzerland, 2, 1879-1880.

[3] WHO (World Health Organization), 1979: Environmental health criteria 14: Ultraviolet radiation. WHO, Geneva, Switzerland

[4] Foyo-Moreno, I., Vida, J., Alados-Arboledas, L., 1998. Ground based ultraviolet (290–385 nm) and broadband solar radiation measurements in south-eastern Spain. Int. J. Climatol. 18, 1389 -1400

[5] Matts PJ. 2006: Solar ultraviolet radiation: definitions and terminology. Dermatol Clin.; 24(1), 1-8.

[6] Weatherhead E.C. and Webb A.R., 1997: International response to the challenge of measuring solar ultraviolet radiation, Radiat Prot Dosim., 72(3-4), 223-229.

[7] Arola, A., Kazadzis, S., Krotkov, N., Bais, A., Gröner, J., Herman, J. R., 2005. Assessment of TOMS UV bias due to absorbing aerosols. J. Geophys. Res., 110, D23211, doi:10.1029/2005JD005913.

[8] Tanskanen, A., Lindfors, A., Maatta, A., Krotkov, N., Herman, J., Kaurola, J., Koskela, T., Lakkala, K., Fioletov, V., Bernhard, J., McHenzie, R., Kondo, Y., O'Neill, M., Slaper, H., Den, P., Bais, A. F., Tamminen. J., 2007. Validation of daily erythemal doses from OMI with ground-based UV measurement data. J. Geophys. Res., 112, D24S44, doi:10.1029/2007JD008830.

[9] Cede, A., Luccini, E., Nuñez, L., Piancetini, R. D., Blumthaler, M., Herman, J. R., 2004. TOMS-derived erythemal irradiance versus measurements at stations of Argentine UV Monitoring Network. J. Geophys. Res., 109, D08109, doi:10.1029/2004JD004519.

[10] Chubarova, N. Y., Yurova, A. Y, Krotkov, N., Herman, J. R, Barthia, P. K, 2002. Comparison between ground measurements of broadband ultraviolet irradiance (300 to 380 nm) and total ozone mapping spectrometer ultraviolet estimates at Moscow from 1979 to 2000. Opt. Eng. , 41, 3070–3081.

[11] Fioletov, V. E., Kimlin, M. G., Krotkov, N., McArthur, L. J. B., Kerr, J. B., Wardle, D. I., Herman, J. R., Meltzer, R., Mathews, T. W., Kaurola. J., 2004. UV index climatology over the United States and Canada from ground based and satellite estimates, J. Geo- phys. Res., 109, D22308. doi:10.1029/ 2004JD004820.

[12] Ialongo, I., Casale, G. R., Siani. A. M., 2008. Comparison of total ozone and erythemal UV data from OMI with ground-based measurements at Rome station. Atmos. Chem. Phys., 8, 3283– 3289. doi:10.5194/acp-8-3283-2008.

[13] Kalliskota, S., Kaurola, J., Taalas, P., Herman, J. R., Celarier, E. A., Krotkov, A., 2000. Comparison of daily UV doses estimated from Nimbus 7/TOMS measurements and ground-based spectroradiometric data. J. Geophys. Res., 105(D4), 5059–5067.

[14] Kazantzidis, A., Bais, A. F., Gröbner, J., Herman, J. R., Kazadizis, S., Krotkov, N., Kyrö, E., Den Outer, P. N., Garane, K., Görts, P., Lakkala, K., Meleti, C., Slaper, H., Tax, R. B., Turunen, T, Zerefos, C. S., 2006. Comparison of satellite-derived UV irradiances with ground-based measurements at four European stations. J. Geophys. Res., 111, D13207, doi:10.1029/2005JD006672.

[15] McKenzie, R. L., Seckmeyer, G., Bais, A. F., Kerr, J. B., Madronich, S., 2001. Satellite retrievals of erythemal UV dose compared with groundbased measurements at northern and southern midlatitudes. J. Geophys. Res., 106, 24051–24062.

[16] Meloni, D., Di Sarra, A., Herman, J. R., Monteleone, F., Piacentino, S., 2005. Comparison of ground-based and total ozone mapping spectrometer erythemal UV doses at the Island of Lampedusa in the period 1998–2003: Role of tropospheric aerosols. J. Geophys. Res., 110, D01202, doi:10.1029/2004JD005283.

[17] Sabburg, J., Rives, J. E., Meltzer, R. S., Taylor, T., Schmalzle, G., Zheng, S., Huang, N., Wilson, A., Udelhofen, P. M., 2002. Comparison of corrected daily integrated erythemal data from the U.S. E.PA/UGA network of Brewer spectroradiometer with model and TOMS-inferred data. J. Geophys. Res., 107(D23), 4676, doi:10.1029/2001JD001565.

[18] Weihs, P., Blumthaler, M., Rieder, H. E., Kreuter, A., Simic, S., Laube, W., Schmalwieser, A. W., Wagner, J. E., Tanskanen, A., 2008. Measurements of UV irradiance within the area of one satellite pixel. Atmos. Chem. Phys., 8, 5615–5626, doi:10.5194/acp8-5615-2008.

[19] Antón, M., Cachorro, V. E., Vilaplana, J. M., Krotkov, N. A, Serrano, A., Badarinath, K. V. S., Kharol, S. K., Kaskaoutis, D. G., Kambezidis, H. D., 2007. Influence of atmospheric aerosols on solar spectral irradiance in an urban area. J. of Atmos. and Solar-Terrest. Phys. 69, 589–599.

[20] Palancar, G. G., Toselli, B. M., 2002. Erythemal ultraviolet irradiance in Córdoba, Argentina. Atmos. Env. 36, 287–292.

[21] Nrmeth, P., Toth, Z., Nagy, Z., 1996. Effect of weather conditions on UV-B radiation reaching the earth's surface. Journal of Photochemistry and Photobiology B: Biology, 32, 177-181.

[22] Frederick, J. E., Snell, H. E., 1990. Tropospheric influence on solar ultraviolet radiation: the role of clouds. Journal of Climate, 3, 373–381.

[23] Ilyas, M., Pandy, A., Jaafar, M. S., 2001. Changes to the surface level solar ultraviolet-B radiation due to haze perturbation. J. Atmos. Chem., 40, 111-121.

[24] Kirchhoff, V. W. J. H., Silva, A. A., Costa, C. A., Leme, N. P., Pavao, H. G. Zaratti, F., 2001. UV-B optical thickness observations of the atmosphere. J.Geophys. Res., 106, 2963-2973.

[25] McArthur, L. J. B., Fioletov, V. E., Kerr, J. B., McElroy, C. T., Wardle, D. I., 1999. Derivation of UV-A irradiance from pyranometer measurements. J. Geophys. Res., 104, 30139-30151.

[26] Di Sarra, A., Cacciani, M., Chamard, P., Cornwall, C., DeLuisi, J.J., Di Iorio, T., Disterhoft, P., Fiocco, G., Fua, D., Monteleone, F., 2002. Effects of desert dust and ozone on the ultraviolet irradiance at the Mediterranean island of Lampedusa during PAUR II. J. Geophys. Res., 107 (D18), 8135, doi:1029/2000JD000139.

[27] Kazadzis, S., Bais, A., Arola, A., Krotkov, N., Kouremeti, N., Meleti, C., 2009. Ozone Monitoring Instrument spectral UV irradiance products: comparison with ground based measurements at an urban environment. Atmos. Chem. Phys., 9, 585–594, doi:10.5194/acp-9-585- 2009.

[28] El-Shazly, S. M., Kassem, Kh. O., Hassan. A. A., Eman, F. E., 2012. An Empirical Model to Estimate UV index in Some Upper Egypt Regions. Resources and Environment 2(5):

216-227 DOI: 10.5923/j.re.20120205.05.

[29] El-Shazly, S. M., Mohamed A. M., Abdel-Azeem, M. A, 1995. A statistical study on weather impaction concerning human well-being in the region of Qena, Egypt. Bull. Fac. Sci., Assuit Univ., 24(1-A), P-P. 189-206.

[30] Kassem, Kh.O., El-Shazzly, S.M., Takahashi, M., Adam, M.E.N, 2009. Variability of surface ozone in some regions in Egypt. Ph. D. Thesis, pp 113-114.

[31] Herman, J. R., Bhartia, P. K., Ziemke, J., Ahmad, Z., Larko, D., 1996. UV-B increases (1979–1992) from decreases in total ozone. Geophys .Res. Lett. 23, 2117–2120

[32] McPeters, R. D., Bhartia, P. K., Krueger, A. J., Herman, J. R., 1998. Earth Probe Total Ozone Mapping Spectrometer (TOMS). Data Products User's Guide. Available at:ftp://toms.gsfc.nasa.gov/pub /eptoms/EARTHPROBE_USERGUIDE.PDF.

[33] McKinlay, A.F., Diffey, B.L. 1987. A reference spectrum for ultraviolet induced erythema in human skin. In Human Exposure to Ultraviolet Radiation: Risks and Regulations; Passchler, W.R., Bosnajokovic, B.F.M., Eds.; Elsevier: Amsterdam, the Netherlands

[34] Fioletov, V. E., Kerr, J. B., Wardle, D. I., Krotkov, N., Herman, J. R., 2002. Comparison of Brewer ultraviolet irradiance measurements with Total Ozone Mapping Spectrometer satellite retrievals. Opt. Eng., 41, 3051-3061.

[35] Torres O., Bhartia P.K., Herman J.R., et al., 1998: Derivation of aerosol properties from satellite measurements of backscattered ultraviolet radiation: theoretical basis. Journal of Geophysical Research, 103, 17,099–17,110.

[36] YES (Yankee Environmental Systems, Inc.), 2008. UVB-1 ultraviolet pyranometer installation and user guide. Available at: ftp://support. yesinc.com /manuals/UVB-1-Manual.pdf.

[37] YES (Yankee Environmental Systems, Inc.), 1997. UVB-1 ultraviolet pyranometer installation and user guide. Version 2.0, pp 3-3 3-4.

[38] Antón, M., Cachorro, V. E., Vilaplana, J. M. Toledano, C., Krotkov, N. A, Arola, A,.Serrano, A., De La Morena, B., 2010. Comparison of UV irradiances from Aura/Ozone Monitoring Instrument (OMI) with Brewer measurements at El Arenosillo (Spain) – Part 1: Analysis of parameter influence. Atmos.Chem. Phys., 10 5979-5989.

[39] NASA (National Aeronautics and Space Administration), 2011. Available at: fttp://toms.gsfc.nasa.gov/pub/eptoms /overpass/.

[40] Bhattarai, B. K., Kjeldstad, B., Thorseth, T. M., Bagheri,. A., 2007. Erythemal dose in Kathmandu, Nepal based on solar UV measurements from multichannel filter radiometer, its deviation from satellite and radiative transfer simulations. Atmos. Res. 85, 112 – 119.

[41] Krotkov, N. A., Bhartia, P. K., Herman, J. R., Fioletov, V., Kerr. J., 1998. Satellite estimation of spectral surface UV irradiance in the presence of tropospheric aerosols: 1. Cloud-free case. J. Geophys. Res., 103(D8), 8779–8793.

[42] Kim J. E., Ryu S. Y. and Kim Y. J., 2008: Determination of radiation amplification factor of atmospheric aerosol from the surface UV irradiance measurement at Gwangju, Korea, Theoretical and Applied Climatology, 91(1-4), 217-228. doi: 10.1007/s00704-006-0285-x.

[43] Hsu, N.C., Herman, J.R., Torres, O., et al., 1999: Comparisons of the TOMS aerosol index with Sun-photometer aerosol optical thickness: results and applications. Journal of Geophysical Research, 104, D6.

[44] Kerr J., Seckmeyer G., Bais A., Blumthaler M., Diaz S., Krotkov N., Lubin D., Madronich S., McKenzie R., Sabzipavar A.A., Verdebout J., 2003: Surface ultraviolet radiation: past, present, and future. Scientific Assessment of Ozone Depletion: 2002, Global Ozone Research and Monitoring Project-Report, 47. World Meteorological Organization, Geneva, Switzerland. Chapter 5.

[45] Silva A. A., 2011: Local cloud cover, ground-based and satellite measurements of erythemal dose rate for an urban, tropical site in Southern Hemisphere, Journal of Atmospheric and Solar-Terrestrial Physics, 73, 2474 –2481.doi:10.1016/j.jastp.2011.09.002.